



# Thermodynamic and thermoeconomic analyses and energetic and exergetic optimization of a turbojet engine

Arman Ekralesian<sup>1</sup> · Fathollah Pourfayaz<sup>1</sup> · Mohammad Hossein Ahmadi<sup>2</sup>

Received: 11 June 2020 / Accepted: 24 September 2020 / Published online: 17 October 2020  
© Akadémiai Kiadó, Budapest, Hungary 2020

## Abstract

In this study, a thermal model for a turbojet engine is proposed. Besides the engine's performance, the cost flow rate of each component is evaluated by performing the energetic, exergetic and exergoeconomic analyses. The compressor pressure ratio ( $\pi_{AC}$ ), flight Mach number (Ma) and turbine inlet temperature (TIT) are three operating variables, which affect the performance of the whole system. Therefore, a sensitivity analysis is carried out to survey the effect of these variables on objective functions (i.e., energy efficiency, exergy efficiency, and exergy destruction). It is found that there are some contradictions between exergy efficiency and exergy destruction, which by increment in TIT energy efficiency increases, while the exergy destruction decreases. Therefore, an optimization should be applied on the presented system. The results show that the highest exergy destruction, unit exergy cost, and cost rate are  $34.96 \text{ GJ h}^{-1}$ ,  $34.85 \text{ US\$ GJ}^{-1}$  and  $437.37 \text{ US\$ h}^{-1}$  occur in the combustion chamber, compressor's outlet flow and combustion chamber outlet stream, respectively. The energetic and exergetic optimization solution is obtained as the Pareto frontier. Final decision-making methods such as TOPSIS, LINMAP are employed for choosing the optimal solution. Design points of LINMAP and TOPSIS having 65.86%, 66.95% thermal efficiency and  $12.51 \text{ GJ h}^{-1}$ ,  $12.65 \text{ GJ h}^{-1}$  exergy destruction, respectively.

**Keywords** Energy · Exergy · SPECO · Exergoeconomic · Sensitivity analysis · Genetic algorithm

## List of symbols

ACC	Annual capital cost rate ( $\text{US\$ h}^{-1}$ )	$k$	Specific heat ratio
$c$	Unit exergy cost ( $\text{US\$ GJ}^{-1}$ )	LHV	Lower heating value of fuel ( $\text{kJ kg}^{-1}$ )
$c_1$	Air inlet speed of system	$m$	Mass flow rate ( $\text{kg s}^{-1}$ )
$c_p$	Specific heat capacity ( $\text{kJ kg}^{-1} \text{K}^{-1}$ )	$n$	Lifetime of the system (year)
$C$	Cost rate ( $\text{US\$ h}^{-1}$ )	$P$	Pressure (kPa)
CRF	Capital recovery factor	PEC	Purchased equipment cost (US\$)
$\dot{E}x$	Exergy rate ( $\text{GJ h}^{-1}$ )	PR	Fuel sell price ( $\text{US\$ kg}^{-1}$ )
IP	Improvement potential	PVF	Present value factor
$f$	Exergoeconomic factor	PW	Present worth (US\$)
$F\dot{C}$	Fuel cost rate ( $\text{US\$ h}^{-1}$ )	$\dot{Q}$	Heat transfer rate (kW)
$h_0$	Specific enthalpy at initial state ( $\text{kJ kg}^{-1}$ )	$R$	Universal gas constant ( $\text{kJ kg}^{-1} \text{K}^{-1}$ )
$h$	Specific enthalpy ( $\text{kJ kg}^{-1}$ )	$s$	Specific entropy ( $\text{kJ kg}^{-1} \text{K}^{-1}$ )
		$s_0$	Specific entropy at initial state ( $\text{kJ kg}^{-1} \text{K}^{-1}$ )
		SV	Salvage value (US\$)
		$T^0$	Total temperature ratio
		$\dot{Z}$	Hourly leveled capital cost rate ( $\text{US\$ h}^{-1}$ )

✉ Fathollah Pourfayaz  
pourfayaz@ut.ac.ir

✉ Mohammad Hossein Ahmadi  
mhosein.ahmadi@shahroodut.ac.ir

<sup>1</sup> Department of Renewable Energy and Environment, Faculty of New Sciences and Technologies, University of Tehran, Tehran, Iran

<sup>2</sup> Faculty of Mechanical Engineering, Shahrood University of Technology, Shahrood, Iran

## Greek symbols

$\pi$	Compression ratio
$\psi$	Exergy efficiency
$\gamma$	Fuel exergy rate
$\eta_{th}$	Thermal efficiency

**Subscripts**

AC	Air compressor
CC	Combustion chamber
chem	Chemical
D	Destruction
f	Fuel
GT	Gas turbine
in	Input
k	The k'th component
kn	Kinetic
out	Output
P	Product
ph	Physical
pt	Potential
a	Dead (reference) state
d	Consumption

**Superscripts**

OM	Operating and maintenance
T	Total
CIC	Capital investment cost

**Introduction**

Gas turbines are employed widely in power generation and aeronautic applications in recent few years. This system is significantly applicable for aviation systems because of its ability to producing great power and high thrust to mass ratio for aircraft [1–3]. The simplest kind of gas turbines are called turbojet engine's (TJE's). It is the basis of other turbojet engines. Turbohaft, turbofan, propfan, and turboprop engines are the advanced types of turbojets [4, 5]. In the past few decades, such advances are made in this regard; however, this technology can still be developed. The motion of the turbojet engine is caused by the acceleration of the working fluid, which typically air is used for this application. The accelerated fluid (i.e., Air) is moving in the reverse direction of the turbojet engine's flight direction, which lead to motion of turbojet engine [6]. The performance of jet engines is the most important feature in the aircraft industries. These systems should be operated economically and efficiently while having the least impact on the environment [7–9]. To make the system compatible with the environment and being cost-effective, system's efficiency should be maximized while the exergy destruction should be decreased. Also the cost rate of systems should be minimized [10, 11]. In recent years, fuel consumption of such systems is increased that is led to entering not only pollutant but also greenhouse gases to the air. This process growing environmental problems. By betterment in the efficiency of fuel utilizing, the environmental effect of emissions can be decreased [12, 13]. Thermodynamic analysis, which is including energy and exergy

analyses can be employed for evaluating the economic and environmental sustainability. In other words, in order to achieve thermodynamics environmental and sustainability constraints, the energy (first law of thermodynamic), and exergy (second law of thermodynamic) analyses can be performed [14–20].

By use of exergy analysis, thermodynamic inefficiencies of the system can be identified. Moreover, exergy destruction of every component of the system can be determined which results in improving the performance of the system or process by decreasing the exergy loss of components [21–25]. According to what is said, exergy analysis is more beneficial than energy analysis. Also the exergy analysis can provide information to reach an ideal system [26]. Exergoeconomic or thermoeconomic evaluation is an engineering subsection that is a combination of economic principles and exergy analysis. Thermoeconomic analysis can provide a beneficial, cost-effective, and affordable information about the system, which cannot achieve by the use of typical energy or exergy or economic analyses separately [27–32]. The exergoeconomic evaluation were applied to various systems to optimize the overall performance of a system including costs and exergy calculations [11]. In the literature, many types of research were conducted for evaluating the exergoeconomic, exergy and energy performances of turbojet engines [33–36]. In [37] exergy analysis was performed on a turbofan engine with afterburner. Exergy destruction and exergy efficiency for each component in an altitude of 11000 meters and at sea level. The resulted exergy efficiency for the four components on the product/fuel basis were obtained 59.9%, 65.6%, 66.7% and 88.5%, meanwhile those for the whole engine at the sea level and an altitude of 11000 m are calculated to be 66.1% and 54.2%. In another study [38] the exergy performance of TJE was studied under various design parameters such as flight Mach number, turbine inlet temperature (TIT), the pressure ratio of compressor, etc. As a result, it was deduced that increasing the Mach number was related to the improvement of exergy efficiency of components and TJE. Balli et al. [39] performed the exergoeconomic and exergy analyses on an aircraft jet engine. The exergy efficiency, unit exergy cost of the jet engine exhaust gases and exergy cost of the engine were calculated to be 34.8% for 2421.9 kW exhaust gases product, 70.96 US\$ GW<sup>-1</sup> and 618.6 US\$ h<sup>-1</sup>, respectively. In the proposed model by Coban et al. [40], exergy and exergoeconomic analyses were applied to the components of the small-scale TJE, which was fueled with biofuel and conventional aviation fuel. Furthermore, the exergy efficiency of components was calculated. The cost rate of thrust was obtained 79.08 US\$ hKN<sup>-1</sup> and 91.89 US\$ hKN<sup>-1</sup> for the conventional jet fuel and biofuel test case.

Many studies were performed on TJE's to identify the optimal point for engine parameters that are mentioned in the literature [41–43]. In [44] a sensitivity analysis was

applied between some conflicting thermodynamic objective functions such as thermal efficiency, propulsive efficiency, specific fuel consumption. Moreover, a Pareto front solution is obtained for the objective function of TJE by employing Genetic algorithm optimization. The comparison results demonstrate the superiority of the new algorithm in preserving the diversity of non-dominated individuals and the quality of Pareto fronts in both two-objective and four-objective optimization processes. In another study [45] a sensitivity analysis was carried out to evaluate the influence of compressor pressure ratio and turbine inlet temperature (TIT) on two-objective functions of study (i.e., specific fuel consumption and specific thrust). Furthermore, a General Algebraic Modeling System was utilized to optimize and analyze the decision variables that aforementioned. The analysis shows that the specific thrust strongly depends on turbine inlet temperature (TIT), where a 10% decrease in TIT results in 6.7% decrease in specific thrust and 6.8% decrease in SFC. Patel et al. [46] for evaluating the influence of some thermodynamic parameters including turbine inlet temperature (TIT), flight Mach number and the pressure ratio of air compressor on the performance of the system, have performed an optimization algorithm. Design points having 70.95% thermal efficiency, 60.23% propulsive efficiency,  $0.0162 \text{ kgs}^{-1} \text{ kN}^{-1}$  specific fuel consumption, and  $1.1666 \text{ kN kg}^{-1} \text{ s}$  specific thrust are obtained during the optimization. Moreover, finding the best solution for the proposed engine employed three decision-making including FUZZY, LINMAP and TOPSIS methods. In the literature, some different analyses, which have been applied on propulsion systems and aero gas turbines, are listed in Table 1.

In the previous investigations, thermodynamic and thermo-economic analyses and energy and exergy optimization are performed separately. In the presented investigation, the exergy, energy, and exergoeconomic analyses alongside an energy, exergy optimization are comprehensively executed on a turbojet engine for the first time, simultaneously.

**Table 1** Some important studies on aircraft and propulsion systems

Aero-engine type	Analysis method	References
Aircraft jet	Energy, exergy, and exergoeconomic	[39]
Turboprop	Exergo-sustainability	[14]
Small-scale turbojet	Energy, exergy, and exergoeconomic	[40]
Turbojet	Energy and exergy	[33, 38]
Turbojet	Exergy	[35]
Turboprop	Conventional and advanced exergy	[7]
Turboprop	Exergy and exergoeconomic	[36]
Turboprop	Energy and exergy	[9]
Turbojet	Energy/optimization	[41, 44, 46]

Generally, the following evaluations are performed on a turbojet engine: The thermodynamic and exergoeconomic analyses are used to reveal the system's efficiencies, inefficiencies and units cost rates. In addition, a detailed parametric analysis is applied to evaluate the influence of various decision variables on exergy and energy efficiencies and exergy destruction. Furthermore, the conflicting objective functions of study (i.e., Thermal efficiency and exergy destruction) are optimized by using a Genetic algorithm optimization approach and the conflict between these two functions is shown in the Pareto front figure. Moreover, LINMAP and TOPSIS decision-making methods are carried out to choose an optimal solution from the Pareto boundary optimal set.

## Thermodynamic analysis

### Assumptions

In this presented investigation, the following assumptions are made [1]:

- The system is working under steady state and steady flow conditions.
- The pressure and temperature of the air at the inlet of the system are 288.15 K and 101.3 kPa, respectively.
- Kerosene is the combustion chamber input fuel and the chemical formula of considered fuel for TJE (Kerosene), and its calorific value is  $C_{12}H_{23}$  and  $43370.596 \text{ kJ kg}^{-1}$ , respectively.
- Friction is negligible, thus pressure loss in the combustion chamber is negligible.
- Kinetic and potential energy and exergy changes through the engine are ignored.
- Chemical exergy of the air is assumed to be close to 0.00.
- The isentropic efficiency of the turbine and compressor, mechanical efficiency of shaft and efficiency of the burner are 0.9, 0.87, 0.98 and 0.8, respectively.
- The inlet air and the products of combustion are assumed to behave as ideal gas and the Specific heats are assumed to be constant.

### Energy analysis

A conventional approach for assessment of jet engine systems is employing the first law of thermodynamics [10]. The inlet total temperature and inlet total pressure of jet engine can be defined by equations as given [47]:

$$P_a^0 = \left(1 + \frac{k-1}{2} * Ma^2\right)^{\frac{k}{k-1}} \quad (1)$$

$$T_a^0 = 1 + \frac{k-1}{2} * Ma^2 \tag{2}$$

And,  $k$  is the specific heat ratio calculated by,

$$k = \frac{c_p}{c_p - R} \tag{3}$$

$c_p$  is specific heat ( $\text{kJ kg}^{-1} \text{K}^{-1}$ ) and  $R$  is universal gas constant ( $\text{kJ kg}^{-1} \text{K}^{-1}$ )

And the air's inlet speed of system is defined as following [48],

$$v_1 = Ma_1 * c_1 \& c_{1} = \sqrt{k * R * T_0} \tag{4}$$

Total pressure and temperature ratio of the compressor is calculated as [4]:

$$P_{AC}^0 = \pi_{AC} \tag{5}$$

$$T_{AC}^0 = 1 + \frac{\pi_{AC}^{\frac{k-1}{k}} - 1}{\eta_{AC}} \tag{6}$$

In the above equations,  $\pi_{AC}$  is the pressure ratio of the air compressor and  $\eta_{AC}$  is compressor isentropic efficiency.

Energy balance equation of combustion chamber can be achieved by using energy conservation.

The fuel–air ratio where  $\dot{m}_f$  and  $\dot{m}_a$  are fuel mass flow and air mass flow, is obtained as follows [49, 50];

$$f = \frac{\dot{m}_f}{\dot{m}_a} = \frac{(c_{pt} * T_3^0 - c_{pc} * T_2^0)}{\eta_b * LHV - c_{pt} * T_3^0} \tag{7}$$

where  $\eta_b$ ,  $c_{pc}$  and  $c_{pt}$  and LHV are the burner's efficiency, specific heat capacity in compressor specific heat capacity in turbine and lower heating value of fuel, respectively.

The total temperature and the pressure ratio in a gas turbine can be found by the following equations [51]:

$$T_{GT}^0 = 1 - \frac{1}{T_3^0} * \frac{c_{pc} * (T_2^0 - T_1^0)}{(1+f) * c_{pt} * \eta_m} \tag{9}$$

$$P_{GT}^0 = \left[ 1 - \left( \frac{1 - \frac{T_4}{T_3}}{\eta_{GT}} \right) \right]^{\frac{k_g}{k_g-1}} \tag{10}$$

where  $T_i^0$ ,  $T_i$ ,  $\eta_{GT}$  are the standard temperature ratio at point  $i$ , temperature at point  $i$  and turbine's isentropic efficiency. The exhaust velocity of the nozzle is given by [48],

$$v_{outlet} = Ma_{outlet} * c_{outlet} \tag{11}$$

where  $is$  are nozzle exit Mach which can be defined as [4],

$$Ma_{outlet} = \sqrt{\frac{2}{k_g - 1} * \left[ \left( \frac{P_{outlet}^0}{P_{outlet}} \right)^{\frac{k_g-1}{k_g}} - 1 \right]} \tag{12}$$

The thrust force ( $F_t$ ) can be calculated by following equation [52]:

$$F_t = \dot{m}_a * ((1+f) * v_{outlet} - v_1) \tag{13}$$

Furthermore the output power of the system is the result of the variation of kinetic energy at the inlet and outlet of the engine. Output power can be computed by the following equation [9]:

$$\dot{W}_{output} = \frac{\dot{m}_a}{2 * 1000} * ((1+f) * v_{outlet}^2 - v_1^2) \tag{14}$$

### Exergy analysis

Figure 1 presents a simplified schematic of the turbojet engine. Exergy is included from physical, chemical, kinetic and potential exergy component that can be determined as follows [53]:

$$\dot{Ex}_D = \dot{m} * (ex_{ph} + ex_{ch} + ex_{kn} + ex_{pt}) \tag{16}$$

For the ideal gas expression, specific physical flow exergy on a mass basis for air and combustion gaseous can be calculated as:

$$ex_{ph} = h - h_0 - T_0 * (s - s_0) \quad \text{or}$$

$$ex_{ph} = c_p * (T - T_0) - T_0 * \left[ c_p * \ln \left( \frac{T}{T_0} \right) - R * \ln \left( \frac{P}{P_0} \right) \right] \tag{17}$$

The specific chemical exergy for liquid fuels with a chemical formula of  $C_xH_yO_zS_n$  is given as [54]:

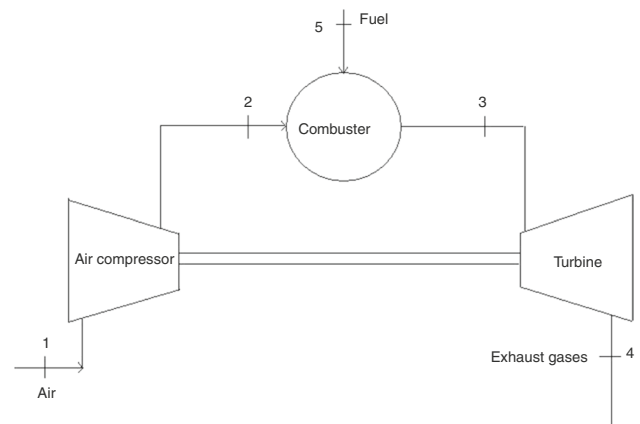


Fig. 1 Simplified schematic of the turbojet engine

$$ex_{ch} = \gamma * LHV \tag{18}$$

where  $\gamma$  is the fuel exergy rate and is given as [55, 56]:

$$\gamma = 1.0401 + 0.01728 * \frac{y}{x} + 0.0432 * \frac{z}{x} + 0.2196 * \frac{n}{x} * \left(1 - 2.0628 * \frac{y}{x}\right)$$

Exergy efficiency and improvement potential are useful functions for appraising the exergetic performance of a system. Exergy efficiency can be calculated as [57, 58]:

$$\psi = \frac{\dot{E}x_p}{\dot{E}x_f} \tag{19}$$

where  $\dot{E}x_p$  and  $\dot{E}x_f$  are the exergy rate of the product and the exergy rate of fuel, respectively, and for each component are presented in Table 3. For total system the product and fuel exergy of the system is calculated by the following equation [52, 59, 60]:

$$\begin{aligned} \dot{E}x_p &= F_t * v_{outlet} \quad \text{and} \\ \dot{E}x_f &= \dot{m} * ex_{ch} + \dot{E}x_{inlet} \end{aligned} \tag{20}$$

where  $\dot{E}x_{inlet}$  is the system inlet exergy.

Improvement potential, which is the rate of exergy destruction minimization through the system, is given below:

$$IP = \dot{E}x_D * (1 - \psi) \tag{21}$$

### Economic analysis

In this study, for obtaining economic parameters of the system, the levelized cost approach is employed. Salvage value (S), present worth (PW) and present value factor (PVF) of the turbojet engine can be determined as following [40, 61]:

$$S = CIC * j \tag{22}$$

$$PW = CIC - S * PWF(i, n) \tag{23}$$

$$PVF = \frac{1}{(1 + i)^n} \tag{24}$$

where  $i, j, n$ , and  $CIC$  are the interest rate, salvage rate, lifetime of the engine and capital investment cost, respectively.

Capital recovery factor (CRF) and annual capital cost of the system (ACIC) also can be written as:

$$CRF = \frac{i * (1 + i)^n}{(1 + i)^n - 1} \tag{25}$$

$$ACIC = PW * CRF(i, n) \tag{26}$$

For every component of the system, the total cost rate can be defined as [62]:

$$\dot{Z}_k^T = \dot{Z}_k^{OM} + \dot{Z}_k^{CIC} \tag{27}$$

where  $\dot{Z}_k^{OM}$  and  $\dot{Z}_k^{CIC}$  are the hourly levelized operating, maintenance, and hourly levelized capital investment cost of each component that can be calculated as [61, 63]:

$$\dot{Z}_k^{OM} = \frac{\dot{C}^{OM}}{\tau} * \frac{PEC_k}{\sum PEC} \tag{28}$$

$$\dot{Z}_k^{CIC} = \frac{ACIC}{\tau} * \frac{PEC_k}{\sum PEC} \tag{29}$$

The levelized fuel cost rate in energy terms ( $F\dot{C}_e$ ) is calculated as [64]:

$$F\dot{C}_e = \frac{PR * \dot{m}_f * 3600 * \tau}{\rho} \tag{30}$$

where  $\rho, \tau$ , and  $PR$  are the density of fuel, the total annual number of hours of system operation at full load and fuel sale price, respectively.  $\dot{C}^f$  is the hourly levelized fuel cost rate in the exergetic term that is given as [64]:

$$\dot{C}^f = \frac{F\dot{C}_e * LHV}{\tau * ex_{ch}} \tag{31}$$

The required economic data for the exergoeconomic analysis are represented in Table 2.

### Exergoeconomic analysis

The exergoeconomic analysis is created by incorporating economic and exergy analyses. Between different approaches which are presented in the literature [65–70], the specific exergy costing approach (SPECOC) is employed in this study

**Table 2** Required economic data for the exergoeconomic analysis [11, 64]

Item	Unit	Value
CIC	(US\$)	1,287,000
OM	(US\$ year <sup>-1</sup> )	99,000
$i$	%	10
$j$	%	15
$N$	year	20
$\tau$	h year <sup>-1</sup>	800
PR	US\$ L <sup>-1</sup>	3

**Table 3** Energy, exergy and exergoeconomic balance equations of the engine's components

Component	Energy and exergy balance	Cost balance and auxiliary equations
Air compressor	$\dot{W}_{AC} + \dot{E}x_1 - \dot{E}x_2 = \dot{E}x_{DAC}$ $\dot{W}_{AC} = \dot{m} * (h2 - h1)$ $\dot{E}x_p = \dot{E}x_2 - \dot{E}x_1 \& \dot{E}x_f = \dot{W}_{AC}$ $\psi_{AC} = \frac{\dot{E}x_2 - \dot{E}x_1}{\dot{W}_{AC}}$	$\dot{C}_{w,Ac} + \dot{C}_1 - \dot{C}_2 + \dot{Z}_{AC}^T = 0$ $c_1 = 0$
Combustion chamber	$\dot{E}x_2 + \dot{E}x_5 - \dot{E}x_3 = \dot{E}x_{DCC}$ $\dot{E}x_p = \dot{E}x_3 \& \dot{E}x_f = \dot{E}x_2 + \dot{E}x_5$ $\psi_{CC} = \frac{\dot{E}x_3}{\dot{E}x_2 + \dot{E}x_5}$	$\dot{C}_5 + \dot{C}_2 - \dot{C}_3 + \dot{Z}_{CC}^T = 0$
Gas turbine	$\dot{E}x_3 - \dot{E}x_4 - \dot{W}_{GT} = \dot{E}x_{DGT}$ $\dot{W}_{GT} = \dot{m} * (h3 - h4)$ $\dot{E}x_p = \dot{W}_{GT} \& \dot{E}x_f = \dot{E}x_3 - \dot{E}x_4$ $\psi_{GT} = \frac{\dot{W}_{GT}}{\dot{E}x_3 - \dot{E}x_4}$	$\dot{C}_{w,GT} + \dot{C}_3 - \dot{C}_4 + \dot{Z}_{GT}^T = 0$ $c_3 = c_2$

due to being simple to apply. According to SPECO method, the cost balance for a given control volume is given as [71–73]:

$$\sum \dot{C}_{in,k} + \dot{Z}_k^T = \sum \dot{C}_{out,k} + \dot{C}_{w,k} \tag{or}$$

$$\dot{C}_{f,k} + \dot{Z}_k^T = \dot{C}_{p,k} \tag{32}$$

where [71, 74],

$$\dot{C}_{in,k} = c_{in,k} * \dot{E}x_{in,k} \tag{33}$$

$$\dot{C}_{out,k} = c_{out,k} * \dot{E}x_{out,k} \tag{34}$$

$$\dot{C}_{W,k} = c_{W,k} * \dot{E}x_{W,k} \tag{35}$$

where  $c_{in,k}$ ,  $c_{out,k}$  and  $c_{W,k}$  are the unit exergy cost for inlet, outlet, and power of  $k$ 'th component of TJE, respectively.

The cost balance and auxiliary equation for components of TJE are mentioned in Table 3.

Exergoeconomic performance parameters including the unit exergy cost of the product ( $c_p$ ), the unit exergy cost of the fuel ( $c_f$ ), exergoeconomic factor ( $f_k$ ) and the cost rate of the exergy consumption rate ( $\dot{C}_d$ ) of TJE and its main equipment are calculated and represented in Table 8. The  $f_k$  parameter can be defined as [75, 76]:

$$f_k = \frac{\dot{Z}_k^T}{\dot{Z}_k^T + \dot{C}_d} \tag{45}$$

### Energetic and exergetic optimization

As discussed in the previous sections, there is a contrast between two considered objective functions and there is just not a unique solution to optimize two functions simultaneously. For this purpose, in this part, a genetic algorithm optimization approach is employed for optimizing target functions.

Multi-objective optimization or multi-criteria optimization is defined as acquiring a vector of decision variables that can be shown  $X^* = [x_1^*, x_2^*, \dots, x_n^*]^T \in \mathcal{R}^n$  to fulfill the constraints [44, 77]. The target functions are:

$$F(X) = [f_1(X), f_2(X), \dots, f_k(X)]^T \in \mathcal{R}^k \tag{36}$$

Which each should be maximized or minimized under  $m$  inequality constraints [44, 77]:

$$g_i(x) \leq 0, \quad i = 1, 2, \dots, m \tag{37}$$

$p$  equality constraints:

$$h_j(x) = 0, \quad j = 1, 2, \dots, p \tag{38}$$

In this between thermal efficiency and the exergy destruction of the system are the conflicting objective functions, which the first should be maximized while the later should be minimized.

In multi-objective optimization, there is a set of optimal solutions instead of a single optimal solution, which is called the Pareto optimal boundary. Pareto approach can be presented by some definition [78].

### Definition Pareto dominance

The vector  $U = [u_1, u_2, \dots, u_k] \in \mathcal{R}^k$  is dominant for vector  $V = [v_1, v_2, \dots, v_k] \in \mathcal{R}^k$  if and only if [44, 77]:

$$\forall i \in \{1, 2, \dots, k\}, u_i \leq v_i \wedge \exists j \in \{1, 2, \dots, k\} : u_i < v_i \tag{39}$$

### Definition of optimal Pareto

A point like  $X^* \in \Omega$  (which  $\Omega$  is an acceptable area in  $\mathcal{R}^k$  that can satisfy 36 and 37 equations) is called Pareto optimal if and only if [44, 77]:

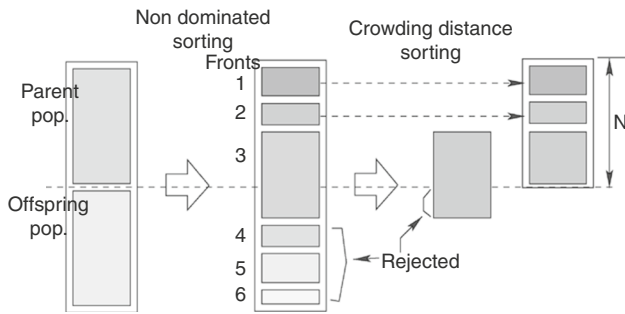


Fig. 2 The basic procedure of NSGAI

$$F(X^*) < F(X) \tag{40}$$

Or in other words:

$$\forall i \in \{1, 2, \dots, k\}, \forall X \in \Omega - \{X^*\} \quad f_i(X^*) < f_i(X) \\ \wedge \exists j \in \{1, 2, \dots, k\} : f_j(X^*) < f_j(X) \tag{41}$$

**Definition of a Pareto set**

In such optimization problems, a Pareto set ( $\Theta^*$ ) is consisting of all design vectors of optimum Pareto. In other words [44, 77]:

$$\Theta^* = \{X \in \Omega | \nexists X' \in \Omega : F(X') < F(X)\} \tag{42}$$

**Definition of Pareto front**

For a given multi-objective optimization problem (MOP), Pareto front or Pareto boundary is a collection of the objective function’s vectors that are made from  $\Theta^*$  and results have no excellence to each other [44, 77].

**Non-dominated Sorting Genetic Algorithm (NSGAI)**

At the First step of this method, the primary population (N) is generated randomly ( $R_1$ ) and the number of members of the population should be constant. After that, the population will be classified and vectors, that can comply with the terms of Eq. (36), will be classified in lower levels. Between these populations, a new random population will be chosen for crossover and mutation. The sum of the newly created population (by applying crossover and mutation) ( $Q_1$ ) and primary population will make the new population and the total new population will be categorized again. As said earlier, the base of NSGAI is that the number of members of the population should be constant while reproduction is ongoing; therefore, in the end, there is an improved population

in higher levels [44, 77]. Figure 2 shows the basic procedure of NSGAI.

To sum up, a flow diagram of Genetic algorithm is presented as following to get a better view about the applied optimization method (Fig. 3).

**Decision-making approaches**

For choosing the final best answers along boundaries, two robust decision-making approaches are used. These methods are included in LINMAP and TOPSIS that are defined by the distance from the ideal and non-ideal point on Pareto front [79, 80]. The ideal point is specified as the point which every objective is optimized separately, irrespective the other ones. The non-ideal point is the point that each objective function has its worst value. The final solution in LINMAP approach, the point with the lowest distance from the ideal point is achieved as the optimum solution. In the TOPSIS approach, the final solution is the point with the farthest distance from the non-ideal point and nethermost distance from the ideal point simultaneously [81–83].

The optimal Pareto boundary for the presented scenario is provided in Fig. 11 and optimal results by applying TOPSIS and LINMAP decision-making approaches are presented in Tables 9 and 10.

**Functions and parameters**

In this study, three operating variables are proposed for optimizing purpose. These parameters including turbine inlet temperature (TIT), the pressure ratio of air compressor  $\pi_c$  and flight Mach number. These variables vary from 1100 K to 1800 K, 5 to 25 and 0 to 1, respectively.

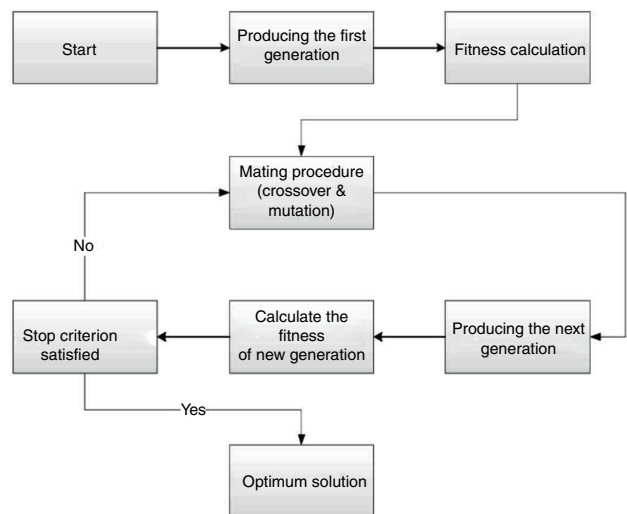


Fig. 3 Flow chart of NSGAI method

**Table 4** Turbojet engine thermodynamic values

State no.	Component	Mass flow/kg s <sup>-1</sup>	Temperature/K	Pressure/kPa
0	Air	14.75	298.15	93.6
1	Compressor inlet	14.75	313.05	111.02
2	Combustor inlet	14.75	487.93	555.14
3	Combustor outlet	15.17	1300.15	555.14
4	Turbine outlet	15.17	1148.50	273.23
5	Fuel	0.42	298.15	93.6

**Table 5** Exergy parameters of the engine's components

Component	Parameters				
	$\dot{E}x_p/\text{GJ h}^{-1}$	$\dot{E}x_p/\text{GJ h}^{-1}$	$\dot{E}x_D/\text{GJ h}^{-1}$	$\dot{I}P/\text{GJ h}^{-1}$	$\psi/\%$
Air compressor	11.21	10.35	0.83	0.064	92.32
Combustion chamber	83.11	48.15	34.96	14.71	57.94
Gas Turbine	12.39	11.43	0.96	0.074	92.25
Total	106.71	69.93	36.78	–	65.55

The energetic and exergetic optimization is employed among the conflicting objective functions. For this aim, Exergy destruction of TJE must be minimized while thermal efficiency must have the maximum value. The output power of the system is the result of the variation of kinetic energy at the inlet and outlet of the engine.

Therefore by dividing the power to net heat, thermal efficiency can be calculated [4],

$$\eta_{th} = \frac{\dot{m}_a * ((1+f) * v_{outlet}^2 - v_1^2)}{2 * 1000 * \dot{m}_f * LHV * \eta_b} \quad (43)$$

In addition,  $\dot{E}x_D$  is the exergy destruction of the TJE that is expressed as below,

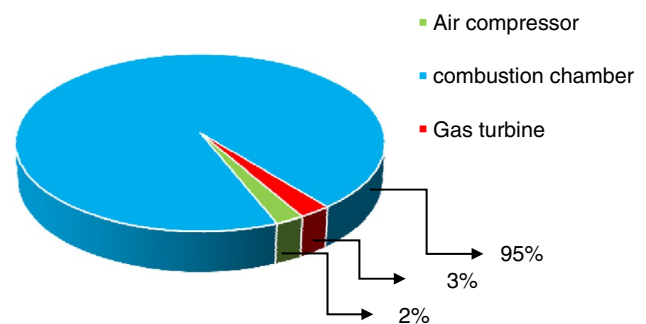
$$\dot{E}x_D = \dot{E}x_{DAC} + \dot{E}x_{DCC} + \dot{E}x_{CGT} \quad (44)$$

## Results and discussion

In this section, the Table 4 is presented which are included from the temperature, the pressure and the mass flow of every state of turbojet engine. These specification are resulted from running the whole cycle with specifying some initial states.

### Exergy analysis

Exergy parameters of engine's components, which is including product and fuel exergy, exergy destruction, improvement potential, and exergy efficiency, are presented in Table 5. As shown in Table 5, the air compressor has the

**Fig. 4** The exergy destruction contribution of components

highest exergy efficiency that is 92.32%. The next rank belongs to the gas turbine and combustion chamber with 92.25% and 57.94%. The total exergy efficiency of the system is obtained 65.55%. In this between combustion chamber has the highest improvement potential, which is 14.71 GJ h<sup>-1</sup>. These all show that the air compressor has the lowest exergy loss and operate in the best condition between different components. In other word, the air compressor converts most the fuel exergy to the product, which is the system's desire. Also the combustor has the highest loss between different components. This high loss could be result of inappropriate utilization of fuel.

Furthermore, the contribution of exergy destruction of each component is shown in Fig. 4. As can be found from the pie chart (Fig. 4), the combustion chamber has the highest exergy destruction with 95% of total exergy destruction of turbojet engine. For minimizing the overall irreversibility, exergy destruction of this component should be decreased.



### Sensitivity analysis per inlet Mach number

Variation of inlet Mach causes a change in the inlet air's speed of the system, therefore the outlet speed of products changes and it generally increases. This variation is bigger than the inlet velocity increment. As given in the methodology section, total work is defined in proportion of the difference between inlet and outlet velocity squared. Therefore total work increases.

Moreover, by variation in the inlet velocity, the fuel-air ratio and as a consequence the system's input heat decreasing. As shown in Fig. 5 and according to what is aforementioned thermal efficiency is increased because of the increment in total work and decrement of input heat with the enhancement of the inlet Mach number.

Moreover, by raising pressure ratio, thermal efficiency firstly increases then decreases. It happens because the turbine inlet pressure and temperature should be proportional to each other. Since the TIT is constant, inlet pressure increment is possible up to a certain value to thermal efficiency increases. After that point, due to low TIT, the kinetic energy of the turbine's inlet compensate lack of this thermal energy. Consequently, outlet speed decreases. So thermal efficiency decreases.

Figure 6 shows curves of the total exergy efficiency of the system, which have an upward trend. By increasing inlet velocity, product exergy of components (such as turbine's work) are increasing. In addition, this increase is more than the increase in the fuel exergy of the components (such as compressor's work) of the system, which is led to increment in exergy efficiency.

Given what is said earlier, by raising Mach number increment in exergy of product is higher than exergy of fuel. Therefore, exergy destruction, which is the difference

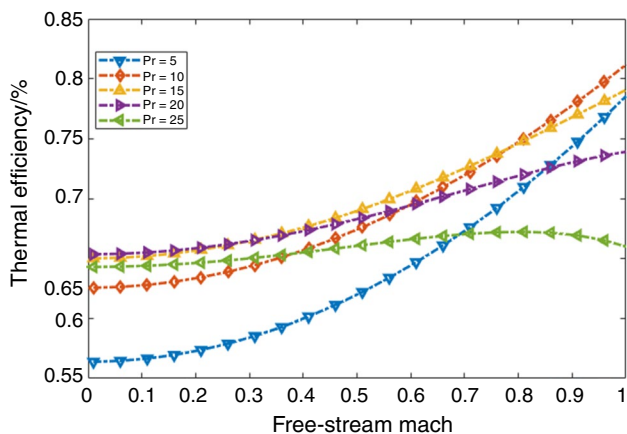


Fig. 5 Variation of thermal efficiency with Mach number and compressor pressure ratio

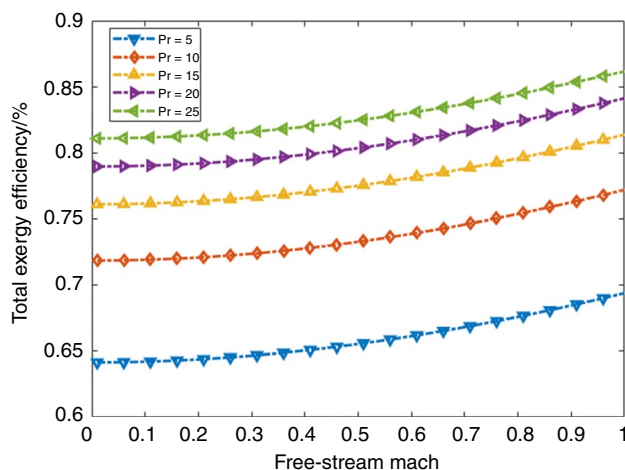


Fig. 6 Variation of exergy efficiency with Mach number and compressor pressure ratio

between these two parameters, generally decreases and is shown in Fig. 7.

### Sensitivity analysis per turbine inlet temperature

First law efficiency increases with rising TIT. This increment happens owing to producing more power in constant compressor's pressure ratio.

As shown in Fig. 8 by an increment in  $\pi_c$  the first law efficiency of the system increases firstly. As mentioned earlier, since TIT and  $\pi_{AC}$  should be proportional to each other. Therefore, by increasing the pressure ratio of the compressor up to 20 and 25, in low TIT values, thermal efficiency drops down. Because low inlet temperature is compensated by the

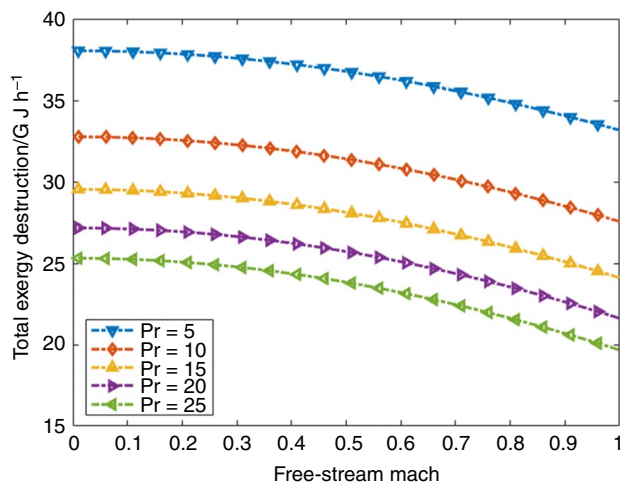
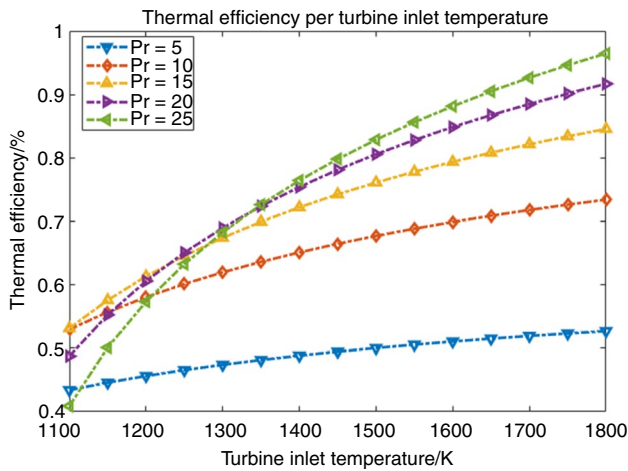


Fig. 7 Variation of exergy destruction with Mach number and compressor pressure ratio



**Fig. 8** Variation of thermal efficiency of system with turbine inlet temperature and compressor pressure ratio

turbine’s inlet kinetic energy and causes decrement in outlet speed, as a result, thermal efficiency of system decreases.

The higher pressure ratio is led to higher turbine inlet pressure that causes more power production. Then by an increase in TIT for a pressure ratio of 20 and 25, thermal efficiency value goes higher than lower pressure ratio’s thermal efficiency system.

As shown in Fig. 9, exergy efficiency curves generally have a downward trend for the same pressure ratio. For higher compression ratio exergy efficiency increases just like [52]. Exergy efficiency is function of outlet speed, thrust force, inlet exergy rate of system and exergy of system. By variation of turbine’s inlet temperature these parameters change differently and in this between the increment

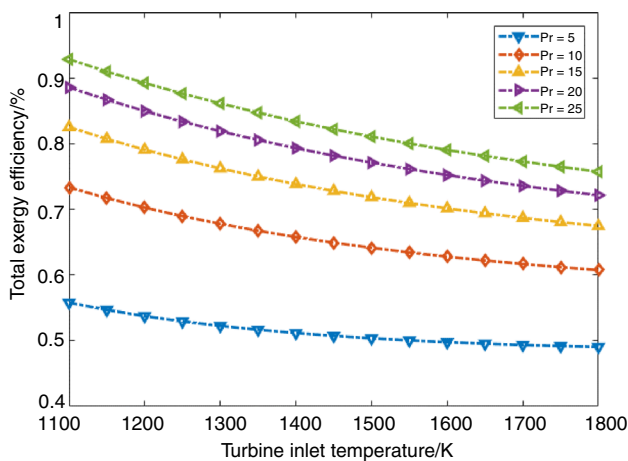


**Fig. 9** Variation of exergy efficiency of system with turbine inlet temperature and compressor pressure ratio

in product exergy is lower than increment in fuel exergy. Therefore by increasing TIT in this system exergy efficiency decreasing.

As presented in Fig. 10, the exergy destruction of TJE cycle is increasing with an increment in TIT in the same compression ratio. Due to augmentation of TIT the irreversibility in the combustion chamber and gas turbine. As a result, exergy destruction increases. By augmentation of compression ratio from 5 to 25, exergy destruction of turbojet engine decreases. As the entropy generation be lower, the input power causes a more pressure ratio in the compressor.

**Exergoeconomic results**

Economic parameters of the turbojet engine and its equipment including purchased equipment cost (PEC), cost rate of the operating and maintenance ( $\dot{Z}_k^{OM}$ ), the hourly leveled total capital investment ( $\dot{Z}_k^{CIC}$ ) and total cost rate ( $\dot{Z}^T$ ) are calculated and presented in Table 6. The  $\dot{Z}_k^{OM}$ ,  $\dot{Z}_k^{CIC}$  and  $\dot{Z}^T$  of system are obtained 123.74 US\$ h<sup>-1</sup>, 184.74 US\$ h<sup>-1</sup> and 314.68 US\$ h<sup>-1</sup>, respectively.

In Table 7, the calculated cost rate and unit exergy cost of every exergy stream and shaft’s work are reported. According to results, the highest cost rate between streams is 437.37 US\$ h<sup>-1</sup> and belongs to the outlet stream of the combustion chamber (stream 3). Furthermore, the outlet stream of the compressor has the highest unit exergy cost with value of 34.85 US\$ GJ<sup>-1</sup>.

The highest value of exergoeconomic factor ( $f_k$ ) belongs to gas turbine and air compressor with a value of 93.36% and 87.19%. These high values reveal that the reason for the high costs is the total cost rate, which is the sum of the

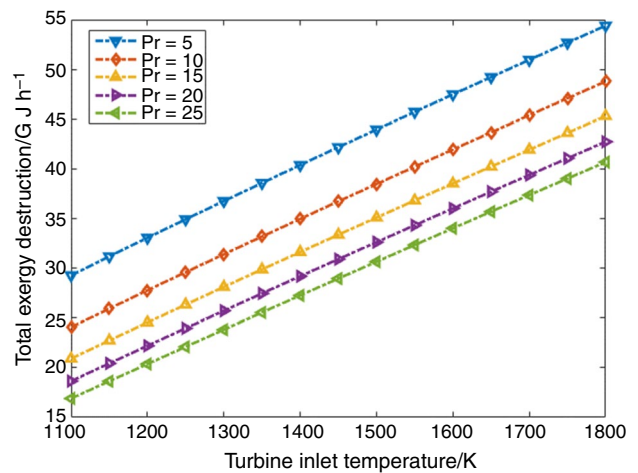


**Fig. 10** Variation of exergy destruction with turbine inlet temperature and compressor pressure ratio

**Table 6** Economic parameters for engine components

Component	PEC/US\$ [11]	$\dot{Z}_k^{CIC}/US\$ h^{-1}$	$\dot{Z}_k^{OM}/US\$ h^{-1}$	$\dot{Z}^T/US\$ h^{-1}$
Air compressor	577500	78.95	55.52	134.48
Combustion chamber	231000	31.58	22.21	53.79
Gas turbine	542850	74.21	52.19	126.41
Total system	1351350	184.74	129.93	314.68

**Table 7** Cost rate and unit exergy cost of exergy streams

State no.	Fluid type/work	$\dot{E}_x/W/GJ h^{-1}$	$\dot{C}/US\$ h^{-1}$	$c/US\$ GJ^{-1}$
0	Air	0	0	0
1	Air	0.79	0	0
2	Air	11.15	388.58	34.85
3	Combustion gases	46.43	437.37	9.42
4	Combustion gases	34.04	320.65	9.42
5	Fuel	71.95	12.27	0.17
-	Compressor work	11.21	256.82	22.91
-	Turbine work	11.43	240.49	21.04

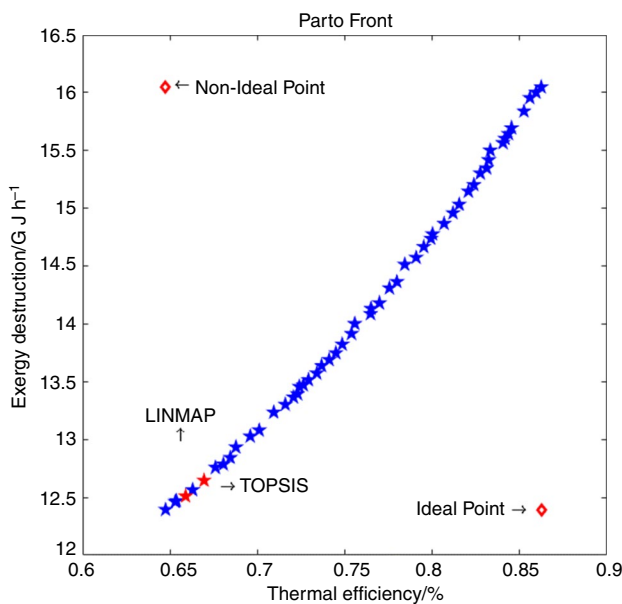


**Fig. 11** Variation of thermal efficiency with exergy destruction of TJE 2-objective optimization

**Table 8** Performance parameters exergoeconomic analysis

Component	$\dot{E}_{x_{des}}/GJ h^{-1}$	$\dot{Z}^T/US\$ h^{-1}$	$c_f/US\$ GJ^{-1}$	$c_p/US\$ GJ^{-1}$	$\dot{C}_d/US\$ h^{-1}$	$f_k/\%$
Air compressor	0.83	134.48	22.91	38.03	19.57	87.19
Combustion chamber	34.96	53.79	35.94	9.42	1256.8	4.11
Gas turbine	0.96	126.41	9.42	21.04	8.98	93.36
Total system	36.78	314.68	68.28	68.49	1285.33	-

operating and maintenance and the capital investment costs. The lowest value of exergoeconomic factor ( $f_k$ ) is 4.11% and belongs to the combustion chamber. This shows that the exergy consumption (that is including exergy destructions and exergy losses) is the result of inappropriate utilization of fuel (Table 8).

**Optimization results**

In this section output results of optimization are proposed. In Fig. 11 Pareto front of two conflicting objective functions is shown. As discussed in previous sections and can be seen in the Pareto front curve, with increment in thermal efficiency exergy destruction increases which generally is not suitable for the system. Therefore with respect to designers targeting, an optimum solution can be chosen from the Pareto front solution.

In this Figure, ideal and non-ideal points are shown. These points have the maximum thermal efficiency with minimum exergy destruction, and minimum thermal efficiency with maximum exergy destruction, respectively. These are applicable for finding decision-making approaches (i.e., LINMAP and TOPSIS) solutions. TOPSIS and LINMAP solutions are defined by the distance from ideal and non-ideal points. As presented in Table 9, LINMAP and TOPSIS solutions are taking place at the point with  $Y_1$  (i.e., thermal efficiency and) value of 0.6589 and 0.6695 and  $Y_2$  (i.e., exergy destruction) value of 12.51 GJ h<sup>-1</sup> and 12.65 GJ h<sup>-1</sup>, respectively. The operating variables (which are TIT,  $\pi_{AC}$  and Mach number) are 1241.72 K, 22.91 kPa and 0.792 for LINMAP and 1250.28 K, 22.94 kPa and 0.798 for TOPSIS.

Also, Table 10 shows the Mean and Maximum value of  $Y_1$  and  $Y_2$  for LINMAP and TOPSIS approaches.

**Table 9** Decision making of optimization results

	$X_1$ /TIT	$X_2$ / $P_r$	$X_3$ /Mach	$Y_1$	$Y_2$
LINMAP	1241.72	22.91	0.792	0.6589	12.51
TOPSIS	1250.28	22.94	0.798	0.6695	12.65
Ref [46]	1638.1	13.4	–	0.6026	–
Ideal point	–	–	–	0.8523	12.39
Non-Ideal point	–	–	–	0.6475	16.05

**Table 10** Mean and Maximum values of decision-making methods

	LINMAP		TOPSIS	
	$Y_1$	$Y_2$	$Y_1$	$Y_2$
Mean	0.6589	12.51	0.6695	12.65
Max	0.6589	12.51	0.6695	12.65

## Conclusions

In the present study, energy, exergy, and exergoeconomic analyses are applied to a turbojet engine's components. These components are consistent with an air compressor, gas turbine, and a combustion chamber. A sensitivity analysis is carried out to reveal the influence of operating variables (i.e., compressor pressure ratio, flight Mach number, and turbine inlet temperature) on objective functions (i.e., energy efficiency, exergy efficiency, and exergy destruction). The variation range of operating variables is between 5 to 25, 0 to 1 and 1100 K to 1800 K. Finally, an energetic and exergetic optimization is performed for finding the optimal points for two of the conflicting objective function (i.e., energy efficiency and exergy destruction). Also by use of LINMAP and TOPSIS decision-making approach, a final optimal solution is chosen.

Some of the main conclusions, which are obtained, are listed as given below:

- The maximum exergy destruction is taking place in the combustion chamber that is  $34.96 \text{ GJ h}^{-1}$ . In addition, the combustion chamber has the highest improvement potential (IP) with a value of  $14.71 \text{ GJ h}^{-1}$ .
- The maximum exergy efficiency between components of the system belongs to an air compressor with a value of 93.39%. The total system exergy efficiency is reached to 65.56%.
- The sensitivity analysis showed that by raising the turbine inlet temperature, exergy destruction and energy efficiency of turbojet engine increases and exergy efficiency decreases.
- The maximum exergy cost and unit exergy cost occurs in the turbine inlet flow and compressor outlet flow.

- The results showed that the final optimal solution of TOPSIS and LINMAP method are 66.95% and 65.89% for thermal efficiency and  $12.65 \text{ GJ h}^{-1}$  and  $12.51 \text{ GJ h}^{-1}$  for exergy destruction, respectively.

The above mentioned results show for improving the function of the proposed TJE, there should be enhancement on combustor efficiency. Because it has the best improvement potential between other components. For instance, the fuel utilization on this component should be improved. Furthermore, the analyses indicate that high turbine's inlet turbine is not proper for system's function. However it increases the thermal efficiency of system, But it increases the exergy destruction that has bad effects on system's performance.

## References

1. Klein D, Abeykoon C, editors. Modelling of a turbojet gas turbine engine. 2015 Internet Technologies and Applications (ITA); 2015 8-11 Sept. 2015.
2. Liu F, William S. Turbojet and turbofan engine performance increases through turbine burners. *J Propul Power*. 2001;17:695–705. <https://doi.org/10.2514/2.5797>.
3. Ekici S, Sohret Y, Coban K, Altuntas O, Karakoc TH. Performance evaluation of an experimental turbojet engine. *Int J Turbo Jet-Engines*. 2017;34:365.
4. El-Sayed AF. Aircraft propulsion and gas turbine engines. Cambridge: CRC Press; 2017.
5. Boyce MP. Gas turbine engineering handbook. New York: Elsevier; 2011.
6. Yucer CT. Thermodynamic analysis of the part load performance for a small scale gas turbine jet engine by using exergy analysis method. *Energy*. 2016;111:251–9. <https://doi.org/10.1016/j.energy.2016.05.108>.
7. Balli O. Advanced exergy analyses of an aircraft turboprop engine (TPE). *Energy*. 2017;124:599–612. <https://doi.org/10.1016/j.energy.2017.02.121>.
8. Zhou D, Zhang H, Weng S. A novel prognostic model of performance degradation trend for power machinery maintenance. *Energy*. 2014;78:740–6. <https://doi.org/10.1016/j.energy.2014.10.067>.
9. Balli O, Hepbasli A. Energetic and exergetic analyses of T56 turboprop engine. *Energy Convers Manag*. 2013;73:106–20. <https://doi.org/10.1016/j.enconman.2013.04.014>.
10. Şöhret Y. A comprehensive approach to understanding irreversibility in a turbojet. *Propul Power Res*. 2018;7(2):129–37. <https://doi.org/10.1016/j.jprr.2018.05.001>.
11. Balli O, Hepbasli A. Exergoeconomic, sustainability and environmental damage cost analyses of T56 turboprop engine. *Energy*. 2014;64:582–600. <https://doi.org/10.1016/j.energy.2013.09.066>.
12. Rosen MA. Assessing energy technologies and environmental impacts with the principles of thermodynamics. *Appl Energy*. 2002;72(1):427–41. [https://doi.org/10.1016/S0306-2619\(02\)00004-1](https://doi.org/10.1016/S0306-2619(02)00004-1).
13. Açıkkalp E, Aras H, Hepbasli A. Advanced exergy analysis of a trigeneration system with a diesel–gas engine operating in a refrigerator plant building. *Energy Build*. 2014;80:268–75. <https://doi.org/10.1016/j.enbuild.2014.05.029>.

14. Aydın H, Turan Ö, Karakoç TH, Midilli A. Exergo-sustainability indicators of a turboprop aircraft for the phases of a flight. *Energy*. 2013;58:550–60. <https://doi.org/10.1016/j.energy.2013.04.076>.
15. Midilli A, Dincer I. Effects of some micro-level exergetic parameters of a PEMFC on the environment and sustainability. *Int J Glob Warm*. 2010. <https://doi.org/10.1504/ijgw.2010.032195>.
16. Yang M, Zhou Y-l, Wang D, Han J, Yan Y. Thermodynamic cycle analysis and optimization to improve efficiency in a 700 °C ultra-supercritical double reheat system. *J Therm Anal Calorim*. 2020;141(1):83–94. <https://doi.org/10.1007/s10973-019-08871-9>.
17. Chopra K, Tyagi VV, Pandey AK. Thermodynamic and techno-economic analysis of heat pipe ETC water heating system for Indian composite climate. *J Therm Anal Calorim*. 2020;139(2):1395–407. <https://doi.org/10.1007/s10973-019-08487-z>.
18. Liu Y, Zhang J, Ju D, Shi L, Han D. Second-law thermodynamic analysis on non-premixed counterflow methane flames with hydrogen addition. *J Therm Anal Calorim*. 2020;139(4):2577–83. <https://doi.org/10.1007/s10973-019-08583-0>.
19. Xu H, Zhang Z, Hu Z, Dai X, Wang J, Jiao W, et al. Thermodynamic and economic analysis of a micro-combined polygeneration system coupled with solar energy and fuels for distributed applications. *J Therm Anal Calorim*. 2020. <https://doi.org/10.1007/s10973-020-09799-1>.
20. Xie H, Yu Q, Zuo Z, Zhang J, Han Z, Qin Q. Thermodynamic analysis of hydrogen production from raw coke oven gas via steam reforming. *J Therm Anal Calorim*. 2016;126(3):1621–31. <https://doi.org/10.1007/s10973-016-5638-9>.
21. Balli O. Advanced exergy analyses to evaluate the performance of a military aircraft turbojet engine (TJE) with afterburner system: splitting exergy destruction into unavoidable/avoidable and endogenous/exogenous. *Appl Therm Eng*. 2017;111:152–69. <https://doi.org/10.1016/j.applthermaleng.2016.09.036>.
22. Kelly S, Tsatsaronis G, Morosuk T. Advanced exergetic analysis: approaches for splitting the exergy destruction into endogenous and exogenous parts. *Energy*. 2009;34(3):384–91. <https://doi.org/10.1016/j.energy.2008.12.007>.
23. Açıkkalp E, Aras H, Hepbasli A. Advanced exergoenvironmental assessment of a natural gas-fired electricity generating facility. *Energy Convers Manag*. 2014;81:112–9. <https://doi.org/10.1016/j.enconman.2014.02.011>.
24. Ajam M, Mohammadi H, Dibae MH, Mohammadi M. Exergy analyzing of a horizontal-axis wind turbine in different conditions based on the BEM method. *J Therm Anal Calorim*. 2020. <https://doi.org/10.1007/s10973-020-10071-9>.
25. Ahmadi B, Golneshan AA, Arasteh H, Karimipour A, Bach Q-V. Energy and exergy analysis and optimization of a gas turbine cycle coupled by a bottoming organic Rankine cycle. *J Therm Anal Calorim*. 2020;141(1):495–510. <https://doi.org/10.1007/s10973-019-09088-6>.
26. Rocco MV, Colombo E, Sciubba E. Advances in exergy analysis: a novel assessment of the Extended Exergy Accounting method. *Appl Energy*. 2014;113:1405–20. <https://doi.org/10.1016/j.apenergy.2013.08.080>.
27. Sahoo PK. Exergoeconomic analysis and optimization of a cogeneration system using evolutionary programming. *Appl Therm Eng*. 2008;28(13):1580–8. <https://doi.org/10.1016/j.applthermaleng.2007.10.011>.
28. Tsatsaronis G. Definitions and nomenclature in exergy analysis and exergoeconomics. *Energy*. 2007;32(4):249–53. <https://doi.org/10.1016/j.energy.2006.07.002>.
29. Ahmadi P, Dincer I. Thermodynamic analysis and thermo-economic optimization of a dual pressure combined cycle power plant with a supplementary firing unit. *Energy Convers Manag*. 2011;52(5):2296–308. <https://doi.org/10.1016/j.enconman.2010.12.023>.
30. Abdollahpour A, Ghasempour R, Kasaiean A, Ahmadi MH. Exergoeconomic analysis and optimization of a transcritical CO<sub>2</sub> power cycle driven by solar energy based on nanofluid with liquefied natural gas as its heat sink. *J Therm Anal Calorim*. 2020;139(1):451–73. <https://doi.org/10.1007/s10973-019-08375-6>.
31. Javadi MA, Hoseinzadeh S, Ghasemiasl R, Heyns PS, Chamkha AJ. Sensitivity analysis of combined cycle parameters on exergy, economic, and environmental of a power plant. *J Therm Anal Calorim*. 2020;139(1):519–25. <https://doi.org/10.1007/s10973-019-08399-y>.
32. Singh G, Singh PJ, Tyagi VV, Barnwal P, Pandey AK. Exergy and thermo-economic analysis of cream pasteurisation plant. *J Therm Anal Calorim*. 2019;137(4):1381–400. <https://doi.org/10.1007/s10973-019-08016-y>.
33. Balli O. Afterburning effect on the energetic and exergetic performance of an experimental turbojet engine (TJE). *Int J Exergy*. 2014;14(2):212–43.
34. Bejan A, Siems DL. The need for exergy analysis and thermodynamic optimization in aircraft development. *Exergy Int J*. 2001;1(1):14–24. [https://doi.org/10.1016/S1164-0235\(01\)00005-X](https://doi.org/10.1016/S1164-0235(01)00005-X).
35. Alihyaei M, Anjiridezfuli A, Rosen M. Exergetic analysis of an aircraft turbojet engine with an afterburner. *Thermal Sci*. 2014. <https://doi.org/10.2298/tsci110911043e>.
36. Karakoc T, Aydın H, Midilli A, Turan O. Exergetic and exergoeconomic analysis of a turboprop engine: a case study for CT7-9C. *Int J Exergy*. 2012. <https://doi.org/10.1504/ijex.2012.049089>.
37. Turgut ET, Karakoc TH, Hepbasli A. Exergetic analysis of an aircraft turbofan engine. *Int J Energy Res*. 2007;31(14):1383–97. <https://doi.org/10.1002/er.1310>.
38. Turan O. Exergetic effects of some design parameters on the small turbojet engine for unmanned air vehicle applications. *Energy*. 2012;46(1):51–61. <https://doi.org/10.1016/j.energy.2012.03.030>.
39. Balli O, Aras H, Aras N, Hepbasli A. Exergetic and exergoeconomic analysis of an Aircraft Jet Engine (AJE). *Int J Exergy*. 2008;5:567–81. <https://doi.org/10.1504/IJEX.2008.020826>.
40. Coban K, Şöhret Y, Colpan CO, Karakoç TH. Exergetic and exergoeconomic assessment of a small-scale turbojet fuelled with biodiesel. *Energy*. 2017;140:1358–67.
41. Noori F, Gorji M, Kazemi A, Nemati H. Thermodynamic optimization of ideal turbojet with afterburner engines using non-dominated sorting genetic algorithm II. *Proc Inst Mech Eng Part G J Aerospace Eng*. 2010;224(12):1285–96.
42. Nariman-zadeh N, Atashkari K, Jamali A, Pilechi A, Yao X. Inverse modelling of multi-objective thermodynamically optimized turbojet engines using GMDH-type neural networks and evolutionary algorithms. *Eng Optim*. 2005;37(5):437–62. <https://doi.org/10.1080/03052150500035591>.
43. Tai V, Chiak See P, Mares C. Optimisation of energy and exergy of turbofan engines using genetic algorithms. *Int J Sustain Aviat*. 2014. <https://doi.org/10.1504/ijsa.2014.062866>.
44. Atashkari K, Nariman-Zadeh N, Pilechi A, Jamali A, Yao X. Thermodynamic Pareto optimization of turbojet engines using multi-objective genetic algorithms. *Int J Therm Sci*. 2005;44(11):1061–71.
45. Najjar YSH, Balawneh IAI. Optimization of gas turbines for sustainable turbojet propulsion. *Propul Power Res*. 2015;4(2):114–21. <https://doi.org/10.1016/j.jprr.2015.05.004>.
46. Patel V, Savsani V, Mudgal A. Efficiency, thrust, and fuel consumption optimization of a subsonic/sonic turbojet engine. *Energy*. 2018;144:992–1002. <https://doi.org/10.1016/j.energy.2017.12.080>.
47. Sforza PM. Chapter 3 - idealized cycle analysis of jet propulsion engines. In: Sforza PM, editor. *Theory of aerospace propulsion*. Boston: Butterworth-Heinemann; 2012. p. 55–126.

48. Dinç A. Sizing of a turboprop unmanned air vehicle and its propulsion system. *J Thermal Sci Technol.* 2015;35:53–62.
49. Tajik Mansouri M, Ahmadi P, Ganjeh Kaviri A, Jaafar MNM. Exergetic and economic evaluation of the effect of HRSG configurations on the performance of combined cycle power plants. *Energy Convers Manag.* 2012;58:47–58. <https://doi.org/10.1016/j.enconman.2011.12.020>.
50. Coban K, Colpan CO, Karakoc TH. Application of thermodynamic laws on a military helicopter engine. *Energy.* 2017;140:1427–36. <https://doi.org/10.1016/j.energy.2017.07.179>.
51. Ji Z, Qin J, Cheng K, Liu H, Zhang S, Dong P. Performance evaluation of a turbojet engine integrated with interstage turbine burner and solid oxide fuel cell. *Energy.* 2019;168:702–11. <https://doi.org/10.1016/j.energy.2018.11.088>.
52. Şöhret Y. Defining the ecological coefficient of performance for an aircraft propulsion system. *Int J Turbo Jet Engines.* 2018;35:171–80. <https://doi.org/10.1515/tjj-2017-0042>.
53. Hepbasli A. A key review on exergetic analysis and assessment of renewable energy resources for a sustainable future. *Renew Sustain Energy Rev.* 2008;12(3):593–661. <https://doi.org/10.1016/j.rser.2006.10.001>.
54. Baklacioglu T, Turan O, Aydin H. Dynamic modeling of exergy efficiency of turboprop engine components using hybrid genetic algorithm-artificial neural networks. *Energy.* 2015;86:709–21. <https://doi.org/10.1016/j.energy.2015.04.025>.
55. Oladiran MT, Meyer JP. Energy and exergy analyses of energy consumptions in the industrial sector in South Africa. *Appl Energy.* 2007;84(10):1056–67. <https://doi.org/10.1016/j.apenergy.2007.02.004>.
56. Balli O. Exergy modeling for evaluating sustainability level of a high by-pass turbofan engine used on commercial aircrafts. *Appl Therm Eng.* 2017;123:138–55. <https://doi.org/10.1016/j.applthermaleng.2017.05.068>.
57. Mehrpooya M, Mousavi SA. Advanced exergoeconomic assessment of a solar-driven Kalina cycle. *Energy Convers Manag.* 2018;178:78–91. <https://doi.org/10.1016/j.enconman.2018.10.033>.
58. Ghorbani B, Mehrpooya M, Mousavi SA. Hybrid molten carbonate fuel cell power plant and multiple-effect desalination system. *J Clean Prod.* 2019;220:1039–51. <https://doi.org/10.1016/j.jclepro.2019.02.215>.
59. Şöhret Y, Dinç A, Karakoç TH. Exergy analysis of a turbofan engine for an unmanned aerial vehicle during a surveillance mission. *Energy.* 2015;93:716–29. <https://doi.org/10.1016/j.energy.2015.09.081>.
60. Dincer I, Rosen MA. Exergy analysis of aircraft flight systems. In: Dincer I, Rosen MA, editors. *Exergy*. 2nd ed. New York: Elsevier; 2013. p. 383–92.
61. Bejan A, Tsatsaronis G, Moran M, Moran MJ. *Thermal design and optimization*. New York: Wiley; 1996.
62. Wu C, Wang S, Li J. Exergoeconomic analysis and optimization of a combined supercritical carbon dioxide recompression Brayton/organic flash cycle for nuclear power plants. *Energy Convers Manag.* 2018;171:936–52. <https://doi.org/10.1016/j.enconman.2018.06.041>.
63. Su W, Li H, Sun B, Li S, Zhang X. Performance investigation on a frost-free air source heat pump system employing liquid desiccant dehumidification and compressor-assisted regeneration based on exergy and exergoeconomic analysis. *Energy Convers Manag.* 2019;183:167–81. <https://doi.org/10.1016/j.enconman.2019.01.004>.
64. Turan O, Aydin H. Exergetic and exergo-economic analyses of an aero-derivative gas turbine engine. *Energy.* 2014;74:638–50. <https://doi.org/10.1016/j.energy.2014.07.029>.
65. Frangopoulos CA. Thermo-economic functional analysis and optimization. *Energy.* 1987;12(7):563–71. [https://doi.org/10.1016/0360-5442\(87\)90097-1](https://doi.org/10.1016/0360-5442(87)90097-1).
66. Tsatsaronis G, Winhold M. Exergoeconomic analysis and evaluation of energy-conversion plants—I. A new general methodology. *Energy.* 1985;10(1):69–80. [https://doi.org/10.1016/0360-5442\(85\)90020-9](https://doi.org/10.1016/0360-5442(85)90020-9).
67. Rosen MA, Dincer I. Exergy–cost–energy–mass analysis of thermal systems and processes. *Energy Convers Manag.* 2003;44(10):1633–51. [https://doi.org/10.1016/S0196-8904\(02\)00179-6](https://doi.org/10.1016/S0196-8904(02)00179-6).
68. Torres C, Valero A, Serra L, Royo J. Structural theory and thermoeconomic diagnosis: Part I. On malfunction and dysfunction analysis. *Energy Convers Manag.* 2002;43(9):1503–18. [https://doi.org/10.1016/S0196-8904\(02\)00032-8](https://doi.org/10.1016/S0196-8904(02)00032-8).
69. Lazzaretto A, Tsatsaronis G. SPECO: a systematic and general methodology for calculating efficiencies and costs in thermal systems. *Energy.* 2006;31(8):1257–89. <https://doi.org/10.1016/j.energy.2005.03.011>.
70. Tsatsaronis G, Lin L, Pisa J. Exergy costing in exergoeconomics. *J Energy Res Technol.* 1993;115(1):9–16. <https://doi.org/10.1115/1.2905974>.
71. Kahraman M, Olcay AB, Sorgüven E. Thermodynamic and thermoeconomic analysis of a 21 MW binary type air-cooled geothermal power plant and determination of the effect of ambient temperature variation on the plant performance. *Energy Convers Manag.* 2019;192:308–20. <https://doi.org/10.1016/j.enconman.2019.04.036>.
72. Hashemi M, Pourfayaz F, Mehrpooya M. Energy, exergy, exergoeconomic and sensitivity analyses of modified Claus process in a gas refinery sulfur recovery unit. *J Clean Prod.* 2019;220:1071–87. <https://doi.org/10.1016/j.jclepro.2019.02.213>.
73. Açikkalp E, Aras H, Hepbasli A. Advanced exergoeconomic analysis of an electricity-generating facility that operates with natural gas. *Energy Convers Manag.* 2014;78:452–60. <https://doi.org/10.1016/j.enconman.2013.11.003>.
74. Bahlouli K. Multi-objective optimization of a combined cycle using exergetic and exergoeconomic approaches. *Energy Convers Manag.* 2018;171:1761–72. <https://doi.org/10.1016/j.enconman.2018.06.100>.
75. Açikkalp E, Aras H, Hepbasli A. Advanced exergoeconomic analysis of a trigeneration system using a diesel-gas engine. *Appl Therm Eng.* 2014;67(1):388–95. <https://doi.org/10.1016/j.applthermaleng.2014.03.005>.
76. Açikkalp E, Zeng T, Ortwein A, Burkhardt H, Klenk W. Exergy, exergoeconomic and enviroeconomic evaluation of a biomass boiler-steam engine micro-CHP system. *Chem Eng Technol.* 2018;41(11):2141–9. <https://doi.org/10.1002/ceat.201800041>.
77. Andalibi MR, Azizi SH, Mohajeri Khameneh P, Abdollahi M. Two and three dimensional optimization of turbojet engine by multi target genetic algorithms. *Aust J Basic Appl Sci.* 2011;5:1594–601.
78. Arslan O. ANN-based determination of optimum working conditions of residential combustors with respect to optimum insulation. *Energy Sources Part A Recov Util Environ Effects.* 2014;36(23):2603–12. <https://doi.org/10.1080/15567036.2011.572133>.
79. Ahmadi MH, Mehrpooya M, Abbasi S, Pourfayaz F, Bruno JC. Thermo-economic analysis and multi-objective optimization of a transcritical CO<sub>2</sub> power cycle driven by solar energy and LNG cold recovery. *Thermal Sci Eng Progress.* 2017;4:185–96. <https://doi.org/10.1016/j.tsep.2017.10.004>.
80. Arslan O, Ergenekon Arslan A, Şentürk Acar M. Multi-Criteria making-decision modeling of b-type ORC-binary geothermal power plant: EATWOS analysis. *Bilecik Şeyh Edebali Univ J Sci.* 2019;6(1):29–48. <https://doi.org/10.35193/bseufbd.561668>.

81. Ahmadi MH, Ahmadi M-A, Maleki A, Pourfayaz F, Bidi M, Açikkalp E. Exergetic sustainability evaluation and multi-objective optimization of performance of an irreversible nanoscale Stirling refrigeration cycle operating with Maxwell-Boltzmann gas. *Renew Sustain Energy Rev.* 2017;78:80–92. <https://doi.org/10.1016/j.rser.2017.04.097>.
82. Arslan, O, Ergenekon Arslan, A, Şentürk Acar, M. (2019). o-Tipi Orc-Binary Jeotermal Güç Santrali Optimizasyonu: Eatwos Analizi. *Bilecik Şeyh Edebali Üniversitesi Fen Bilimleri Dergisi* 6, 222–236. <https://doi.org/10.35193/bseufbd.601745>.
83. Arslan AE. Multi-criteria decision making of simav integrated geothermal energy system: AHP-Eatwos hybrid analysis. *Curr Res Hum Soc Sci.* 2020;1:83.

**Publisher's Note** Springer Nature remains neutral with regard to jurisdictional claims in published maps and institutional affiliations.